Acta Cryst. (1996). D**52**, 738–742

Crystallization and Preliminary X-ray Diffraction Studies of New Crystal Forms of *Escherichia coli* P_{II} Complexed with Various Ligands

KAREN J. EDWARDS,* PETER M. SUFFOLK, PAUL D. CARR, MICHAELA WEGMAN, EONG CHEAH, AND DAVID L. OLLIS

Centre for Molecular Structure and Function, Research School of Chemistry, Australian National University, GPO Box 414, Canberra, ACT 2601, Australia. E-mail: karen.edwards@anu.edu.au

(*Received 6 December 1995; accepted 5 March 1996*)

Abstract

New crystals of the signal-transducing protein P_{II} have been obtained in the presence of a number of different effector ligands. Various crystal forms are observed depending on the nature of the ligand(s). Co-crystallization with 2-ketoglutarate, glutamate and pyrophosphate produces hexagonal crystals similar to the wild type, ATP yields cubic crystals and ATP in conjunction with 2-ketoglutarate or glutamate yields orthorhombic crystal forms. All of the above crystals have been characterized by X-ray diffraction analysis. The hexagonal crystals belong to space group $P6_3$, cubic crystals to either $I23$ or $I2_13$ and orthorhombic crystals to $I222$. A molecular-replacement solution for the P_{II}/ATP/2-ketoglutarate crystals has been obtained giving us an initial model for a trimer in the orthorhombic crystal form.

1. Introduction

Glutamine synthetase (GS) is a key enzyme involved in the uptake of nitrogen by *E. coli* and related bacteria. Both the activity of the enzyme and transcription of its gene (*glnA*) are highly regulated in response to environmental levels of nitrogen (for review see Magasanik, 1993). P_{II} is a signal-transduction protein that plays a key role in the regulation of GS by controlling the function of the enzymes adenylyltransferase (ATase) and the nitrogen regulatory protein II (NR_{II}).

P_{II} is an indicator of nitrogen sufficiency and depending on levels of cellular nitrogen has uridine monophosphate (UMP) groups added or removed by the uridylyltransferase/uridylyl-removing bifunctional complex (UTase/UR). When levels of cellular nitrogen are low, increased activity of GS is required (Magasanik, 1993). In the presence of adenine triphosphate (ATP) and 2-ketoglutarate uridylylation of P_{II} is greatly enhanced (Kamberov, Atkinson, Feng, Chandran & Ninfa, 1994). UMP is covalently bound at residue Tyr51 in a reaction catalyzed by UTase/UR (Son & Rhee, 1987). Uridylylated P_{II} (P_{II}-UMP) binds to ATase to effect increased deadenylylation and thus activation of the GS dodecamer. In parallel with this process, NR_{II}, in the absence of P_{II}, acts as a kinase phosphorylating the nitrogen regulatory protein I (NR_I) to yield increased transcription of *glnA*.

Under conditions of high cellular nitrogen the same levels of GS activity are not required and subsequently the uridylyl-removing function of UTase/UR is activated by glutamine thus maintaining high levels of unmodified P_{II} (Kamberov *et al.*, 1994). P_{II} then interacts with ATase to bring about increased adenylylation and subsequent deactivation of GS. Unmodified P_{II} also binds to NR_{II} activating dephosphorylation of NR_I and thereby reducing transcription of *glnA* . This binding is greatly enhanced in the presence of ATP and 2-ketoglutarate (Kamberov, Atkinson & Ninfa, 1995).

Unliganded P_{II} crystals are hexagonal and belong to the $P6_3$ space group. The structure of unliganded *E. coli* P_{II} has been solved (Cheah *et al.*, 1994) and refined to 1.9 Å resolution (Carr, Cheah *et al.*, 1996). It is shown to be a compact trimer consisting of three tightly interlocking β-sheets surrounded by α-helices. Functionally important regions appear to reside in a number of flexible surface loops emanating from a stable core region and also a cleft formed between neighbouring monomers. One of these loops, the T loop, is involved in crystal contacts in the unliganded structure of P_{II}. Recent biochemical evidence suggests an important role for small-molecule ligands in effecting allosteric changes in P_{II} (Kamberov *et al.*, 1995). ATP, 2-ketoglutarate and glutamate have all been shown to bind to P_{II}. ATP and 2-ketoglutarate bind tightly with apparent binding constants in the micromolar range whilst glutamate binds more weakly. These ligands are necessary to be bound for uridylylation of P_{II} by UTase/UR. They also enhance the binding of P_{II} to NR_{II} to form the complex that controls adenylylation of GS. Inspection of the unliganded structure shows that the loop and cleft regions may be potential sites for ligand binding whilst the interlocking β-sheet core gives the structure stability. The binding of ligands may also stabilize the T loop in a suitable conformation for interaction with uridylyl transferase.

In order to elucidate the potential structural changes, P_{II} has been crystallized with a number of different ligands including 2-ketoglutarate (2-KG), glutamate, ATP and pyrophosphate (PP*i*), and ATP in combination with 2-ketoglutarate and glutamate. The latter was carried out

Table 1. *Crystallization and characterization of P_{II}/ligand crystals*

Crystal	Ligand(s)	Crystallization conditions†	Cell (Å)	Space group	V_m (Å^3 Da^{-1}) (No. of molecules/AU)
Hexagonal					
native		1.0 *M* NaCl, 1.0 *M* phosphate, pH 7.0	61.6 56.3	$P6_3$	2.49 (1)
PII1	2-KG	1.0 *M* AS, 0.2 *M* NaCl 0.1 *M* CHES, pH 9.5	61.2 58.8	$P6_3$	2.56 (1)
PII2	PP*i*	1.2 *M* AS, 0.2 *M* NaCl 0.1 *M* CHES, pH 9.5	60.9 58.9	$P6_3$	2.54 (1)
PII3	Glutamate	1.8 *M* AS, 0.3 *M* NaCl 0.1 *M* CHES, pH 9.5	61.6 59.0	$P6_3$	2.61 (1)
Cubic					
PII4	ATP	1.1–1.5 *M* AS, 8–10%(*v*/*v*) glycerol 0.1 *M* Tris, pH 8.0–9.0	89.7	$I23$ ($I2_13$)	2.43 (1)
Orthorhombic					
PII5a*	ATP/2-KG	0.16–0.2 *M* NaOAc 21–24% PEG 3400 0.1 *M* HEPES, pH 7.5	88.5 88.4 91.8	$I222$	2.41 (3)
PII5b*			87.8 87.6 91.4	$I222$	2.36 (3)
PII6	ATP/ glutamate	0.2 *M* NaOAc, 21% PEG 3400 0.1 *M* HEPES, pH 7.5	88.7 89.1 92.6	$I222$	2.46 (3)

* PII5a and PII5b crystals are grown under the same conditions. † AS = ammonium sulfate, NaOAc = sodium acetate.

Table 2. *Data-collection statistics for P_{II}/ligand crystals*

Crystal*	Resolution (Å)	No. of reflections	No. of unique reflections	R_{merge}† (%)	Completeness of data (%)	Temperature (K)
PII1	2.5	41550	8349	6.5	85	277
PII2	2.0	44793	9164	5.8	89	277
PII4	3.0	7676	2310	12	95	277
PII5a	2.3	34808	15970	8.0	79	277
PII5b	2.1	71128	20930	5.2	94	100

* PII6 is not included in this table as it suffered radiation damage before a worthwhile data set could be collected. † $R_{merge} = \sum |I - \langle I \rangle| \sum I$.

using both uridylylated and un-uridylylated P_{II}. The preliminary X-ray diffraction analysis results are presented here and also the molecular-replacement solution of P_{II} complexed with ATP and 2-ketoglutarate.

2. Experimental

2.1. *Crystallizations*

P_{II} was purified as previously described (Vasudevan *et al.*, 1994) and stored in 20 m*M* Hepes, 1 m*M* β-mercaptoethanol, 1 m*M* EDTA and 20 m*M* spermidine at pH 7.5. All crystals were grown using the hanging-drop method (McPherson, 1990) by mixing equal volumes of protein solution (18–25 mg ml^{-1}) containing the appropriate ligand(s) with the relevant reservoir solution at 277 K. Table 1 describes the crystallization conditions and overall morphology of the co-crystals. Crystals required 3–4 weeks to grow to optimum size.

2.2. *X-ray data collection*

All X-ray data were collected on a Rigaku R-AXIS IIC image-plate detector mounted on a Rigaku RU 200 rotating-anode X-ray generator operating at 50 kV and 100 mA. Data were collected at 277 K with the exception of the second P_{II}/ATP/2-KG data set (P_{II}5b) which was collected at 100 K. Unit-cell dimensions were determined from still images using the software supplied with the R-AXIS IIC image-plate detector (Sato, Yamamoto, Katasumi, Tanaka & Higashi, 1992) and are given in Table 1. Data-collection statistics are summarized in Table 2. P_{II}/ATP/2-KG crystals were prepared for cryocooling as follows: crystals were first transferred to a stabilizing solution consisting of 24% polyethylene glycol (PEG) 3400, 0.2 *M* sodium acetate at pH 7.5 and then transferred to the cryoprotectant buffer containing 24% PEG 3400, 0.2 *M* sodium acetate and 10%(*v*/*v*) glycerol at pH 7.5. After two washes

in the cryoprotectant solution the crystals were then flash cooled in hair loops using a modified Molecular Structure Corporation cryocooling system (Carr, Barlow *et al.*, 1996).

2.3. *Molecular-replacement solution of P_{II}/ATP/2-KG*

All calculation were performed using *X-PLOR* version 3.1 (Brünger, 1992) running on a Fujitsu VP 2200 computer. The initial molecular-replacement (MR) solution for P_{II}/ATP/2-KG was solved using the P_{II}5a data set collected at 277 K.

2.4. *Self-rotation search*

V_m (Matthews, 1968) calculations indicated the presence of three molecules in the asymmetric subunit. A self-rotation search was performed to locate the non-crystallographic symmetry (NCS) relating the three molecules within the asymmetric unit. A native Patterson map was calculated on a 1.0 Å grid using 1246 reflections with $F > 2\sigma(F)$ between 10.0 and 5.0 Å from data set P_{II}5a. Vectors within a shell of radius 5.0–30.0 Å were used. The self-rotation search was performed by varying ψ and φ in 2° steps in the range 0–180° while κ was varied between 110–130 and 160–180°.

2.5. *Cross-rotation search*

A search model for MR was constructed by generating the P_{II} trimer and removing the T and B loops (residues 37–55 and 82–89, respectively) from the 1.9 Å refined coordinates. The model Patterson was computed by placing the search model in a *P*1 cell with dimensions 130

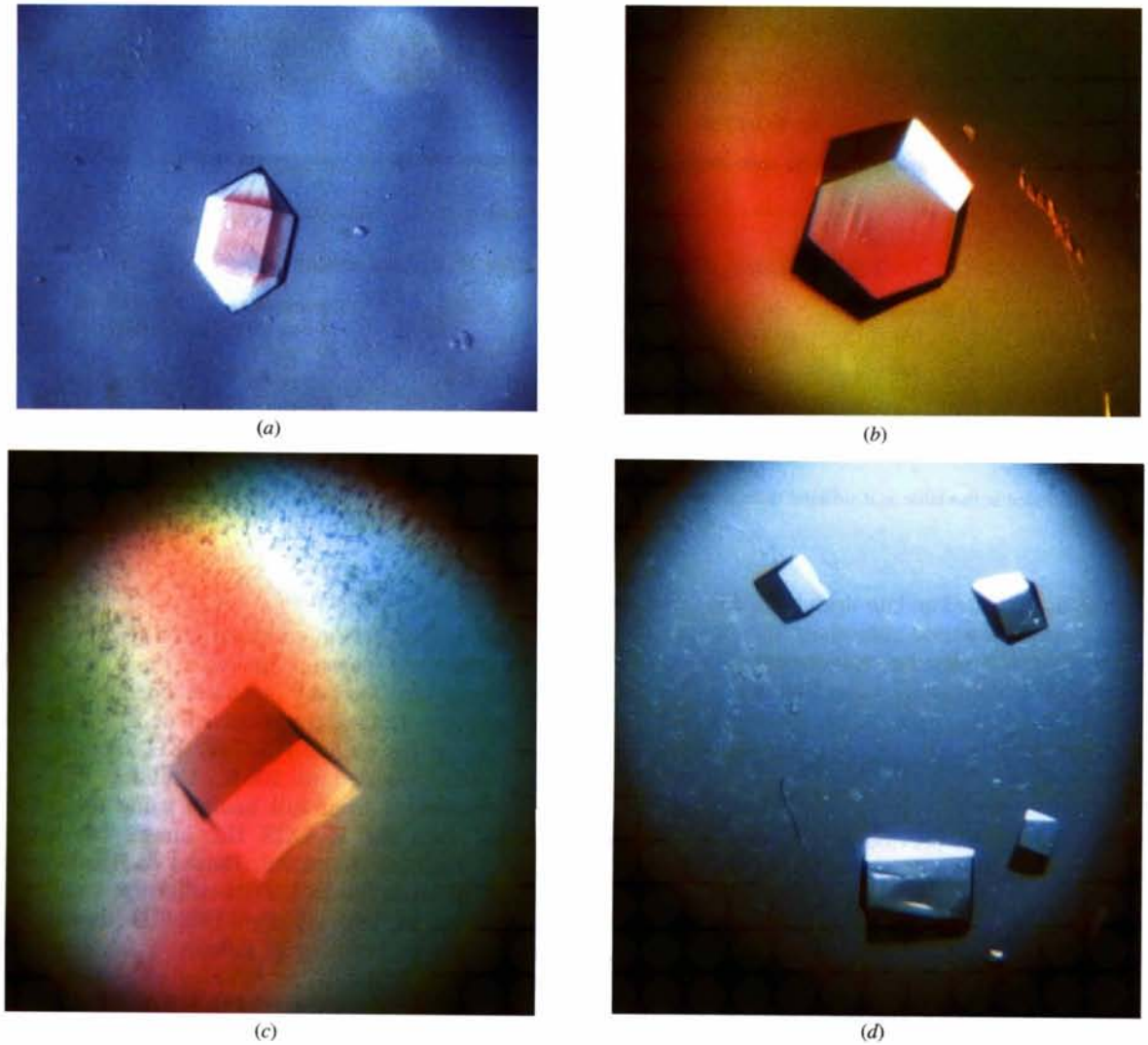

Fig. 1. Range of crystal morphologies observed for P_{II} complexed with various ligands. (*a*) P_{II} native – hexagonal, (*b*) P_{II} complexed with 2-ketoglutarate – hexagonal, (*c*) P_{II} complexed with ATP – cubic and (*d*) P_{II} complexed with ATP and 2-ketoglutarate – orthorhombic.

× 130 × 130 Å and $\alpha = \beta = \gamma = 90°$. Patterson vectors within a shell of radius 5.0–30.0 Å and 2588 reflections with $F > 2\sigma(F)$ between 10.0 and 4.0 Å were used. Patterson vectors were rotated using the Eulerian angles (θ_1, θ_2, θ_3) (Rossman & Blow, 1962). The asymmetric unit of rotational space, $0 \leq \theta_1 \leq 2\pi$, $0 \leq \theta_2 \leq \pi/2$, $0 \leq \theta_3 \leq \pi$ (Rao, Jih & Hartsuck, 1980) was searched using an angular grid interval of 2.5°.

2.6. *Patterson correlation refinement*

Patterson correlation (PC) refinements were performed on all the solutions from the cross-rotation search and carried out in the resolution range 10.0–4.0 Å. The PC refinement consisted of 15 steps of rigid-body optimization for the trimer followed by 25 steps of rigid-body optimization defining each monomer as a separate group.

2.7. *Translation search*

Translation searches were performed using the three highest PC-refined solutions in the *I*222 and $I2_12_12_1$ space groups. Data with $F > 2\sigma(F)$ between 10.0 and 4.0 Å were included for the translation search. The asymmetric unit for the translation search was $x = 0$–0.5, $y = 0$–0.5, $z = 0$–0.5 (Hirshfeld, 1968) with a step size of 0.02 fractional units. The translation search solutions were then subjected to rigid-body refinements initially in the range 10.0–4.0 Å (2588 reflections) and then 8.0–3.0 Å (6140 reflections).

3. Results and discussion

Cell dimensions for the various crystals are given in Table 1. The hexagonal crystal forms all belong to space group $P6_3$ and generally diffract to better than 2.0 Å. The cubic crystal form belongs to space group *I*23 or $I2_13$ and diffracts to *ca* 3.0 Å resolution. These crystals exhibit high mosaic spread and the data has higher merging statistics than any of the other crystal forms. The orthorhombic crystals belong to space group *I*222 and although they diffract to *ca* 2.3 Å resolution at 277 K they exhibit decay because of radiation damage during the course of the data collection. Flash-cooling of these crystals to 100 K resulted in crystals which were stable in the X-ray beam and showed no signs of radiation damage after 12 d. This enabled a more complete (94%) data set to be collected with improved R_{merge} statistics. There was an approximate 2% reduction in cell volume as a result of cryocooling.

Co-crystallization of P_{II} with the various ligands, either singly or in combination, results in markedly different crystal morphologies which appear under a wide range of different conditions (Fig. 1). As a comparison, native, unliganded P_{II} crystals are grown at pH 7.0 with hexagonal morphology. The 2-KG, PP*i*, and glutamate ligand crystals grow at higher pH than the native crystals (Table 1), are also hexagonal and are similar to the native crystals. A native data set has been collected for an unliganded crystal which was sequentially soaked from pH 7.0 to pH 9.5 and difference maps calculated (Suffolk, 1995, data not shown) to compare the high-pH data set to the original native. There are no significant differences between the models from the native and high-pH data sets and we conclude that any differences in the crystal structures of the ligand bound crystals will be a direct result of ligand binding. Control experiments were performed to assess whether unliganded P_{II} would crystallize under the ligand-bound conditions. All results were negative. Inspection of electron-density maps calculated from difference Fourier calcualtions performed on the ligand-bound data sets do not readily give the positions of loop regions or ligands. This is consistent with conformational changes occurring upon binding of ligands to P_{II} especially in the large T-loop region of the molecule.

Crystals grown in the presence of ATP are cubic and show no birefringence. Crystals grown with ATP in combination with either 2-KG or glutamate exhibit slight birefringence and are orthorhombic. It is interesting to note the effect of the various ligands on the cell and space group of the crystals. Crystallization of P_{II} with both ATP and 2-KG or glutamate results in a small but perceptible change in the cell from cubic to orthothombic. Co-crystallization experiments with ATP fail to produce crystals with the same morphology and space group as the unliganded form of P_{II}. This lends support to the idea that the T loops may have undergone a conformational change upon ligand binding disrupting the crystal contacts which were present in the unliganded crystal form.

A molecular-replacement (MR) solution has been found for the P_{II}/ATP/2-KG crystals (P_{II}5a). The self-rotation function produces a strong peak at $\psi = 54.6$, $\varphi = 44.8$, $\kappa = 120°$ which is consistent with the presence of a threefold non-crystallographic symmetry element. Results from the cross-rotation function gave three prominent peaks which were related by the non-crystallographic symmetry of the search molecule. PC refinement also resulted in three related peaks of equal weight which were significantly higher than the other peaks. Results from the translation search gave three solutions related by the non-crystallographic symmetry of the molecule. Results for the solution which was used for further refinement are as follows. Rotation function [$\theta_1 = 70.0$, $\theta_2 = 60.0$, $\theta_3 = 132.5$, rotation-function (RF) value = 9.28]; PC refinement ($\theta_1 = 71.1$, $\theta_2 = 659.6$, $\theta_3 = 133.2$, PC value = 0.15); translation function [$u = 0.36$, $v = 0.16$, $w = 0.04$, $TF_{max} = 0.36$, $TF_\sigma = 0.03$, $R_{TF} = 49$ % (8–3.5 Å)]; rigid-body minimization, $R_{RB} = 41.8\%$ (8–3 Å). A translation search in the $I2_12_12_1$ space group gave significantly higher (*ca* 6%) *R* factors than those performed in *I*222. The packing for the P_{II} trimer in the asymmetric unit was examined

and judged to be satisfactory. A positional refinement in the range 8.0–3.0 Å (6140 reflections) gave an *R* factor of 32.4%. At this stage the cryocooled data set (P_{II}5b) became available and the model above was fitted to the new data by rigid-body refinement in the resolution range 8.0–3.0 Å (6817 reflections) to give an *R* factor of 34.3%.

The structural refinements of the various liganded forms of P_{II} are currently underway. We anticipate that these structure determinations will provide us with new insights into the way P_{II} influences the enzymes involved in nitrogen regulation and how its interaction with various ligands plays a crucial role in signal transduction.

The ANU Supercomputer Facility is thanked for making computer facilities available to us on their Fujitsu VP2200 computer by a grant of time on the machine.

References

Brünger, A. T. (1992). *X-PLOR Version* 3.1. *A System for X-ray Crystallography and NMR*. Yale University, Connecticut, USA.

Carr, P. D., Barlow, P. J., Barton, J. D., Edwards, K. J., Pepper, D. C., Ritherdon, C. & Ollis, D. L. (1996). *J. Appl. Cryst.* In the press.

Carr, P. D., Cheah, E., Suffolk, P. M., Vasudevan, S. G., Dixon, N. E. & Ollis, D. L. (1996). *Acta Cryst.* D**52**, 93–104.

Cheah, E., Carr, P. D., Suffolk, P. M., Vasudevan, S. G., Dixon, N. E. & Ollis, D. L. (1994). *Structure*, **2**, 981–990.

Hirshfeld, F. L. (1968). *Acta Cryst.* A**24**, 301–311.

Kamberov, E. S., Atkinson, M. R., Feng, J., Chandran, P. & Ninfa, A. J. (1994). *Cell. Mol. Biol. Res.* **40**, 175–191.

Kamberov, E. S., Atkinson, M. R. & Ninfa, A. J. (1995). *J. Biol. Chem.* **270**, 1–11.

McPherson, A. (1990). *Eur. J. Biochem.* **189**, 1–23.

Magasanik, B. (1993). *J. Cell. Biochem.* **51**, 34–40.

Matthews, B. W. (1968). *J. Mol. Biol.* **33**, 491–497.

Rao, S. N., Jih, J.-H. & Hartsuck, J. A. (1980). *Acta Cryst.* A**36**, 878–884.

Rossmann, M. G. & Blow, D. M. (1962). *Acta Cryst.* **15**, 24–31.

Sato, M., Yamamoto, M., Katasumi, I., Tanaka, N. & Higashi, T. (1992). *J. Appl. Cryst.* **25**, 348–357.

Son, H. S. & Rhee, S. G. (1987). *J. Biol. Chem.* **262**, 8690–8695.

Vasudevan, S. G., Gedye, C., Dixon, N. E., Cheah, E., Carr, P. D., Suffolk, P. M., Jeffrey, P. D. & Ollis, D. L. (1994). *FEBS Lett.* **337**, 255–258.